2009 American Control Conference
Hyatt Regency Riverfront, St. Louis, MO, USA
June 10-12, 2009

Improved Part Quality in Stamping Using Multi-Input Multi-Output (MIMO) Process Control

Yongseob Lim, Ravinder Venugopal, and A. Galip Ulsoy

Abstract— The binder force in sheet metal forming controls the material flow into the die cavity, and maintaining precise material flow characteristics is crucial for producing a high-quality stamped part. Process control can be used to adjust the binder force based on tracking a reference punch force trajectory to improve part quality and consistency. The purpose of this paper is to present a systematic approach to the design and implementation of a suitable MIMO process controller. The approach includes modeling of the sheet metal forming process, and the design of the process controller based on simulation. Experimental results from a complex-geometry part show that the MIMO process controller, designed through simulation, is effective.

I. INTRODUCTION

1.1 Background

Sheet metal stamping is one of the primary manufacturing processes, because it allows stamped parts, such as automotive body panels and fuel tanks, to be produced in large volumes at high-speed and with low-cost. A stamped part is made by placing a sheet of metal between an upper die (or punch) and a lower die, which are geometric negatives of each other, and then stamping the sheet of metal using a press. Fig. 1 shows a schematic of a simplified stamping process. The basic components are a punch, die, and a set of blank holders (or binders) which may, or may not, include drawbeads around the edges of the dies. The punch draws the sheet metal blank to form the desired shape while the blank holder controls the flow of sheet metal into the die cavity. Some process variables are shown in this figure: F_p is the punch force, l_s is the draw-in, h is the punch stroke, F_b is the binder force, and F_r is the restraining force within the blank.

Once die design and validation are accomplished, high productivity is the hallmark of stamping operations due to their suitability for large volume production. Stamping presses typically feature a large mechanism (the press ram) that forces the punch, or upper die, towards the lower die, with the material to be drawn placed in between. Traditionally, stamping presses have been mechanical in design, but more modern presses are often electro-hydraulic. Typical presses also have rubber, springs, and pneumatic/hydraulic pistons to cushion the die in a stamping press from the punch impact.

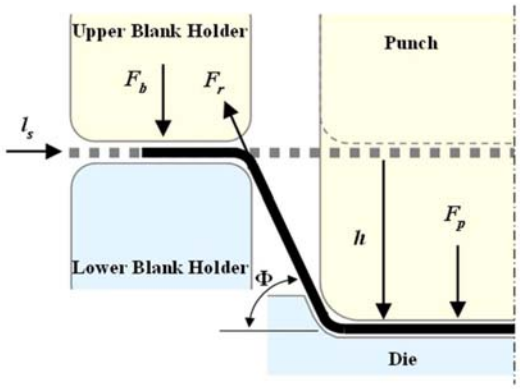

Fig. 1: Schematic of a sheet metal forming process.

The main quality considerations in stamping are formability (e.g., the ability to avoid wrinkling caused by excessive local compression, and tearing caused by excessive local tension) and dimensional accuracy (e.g., reduction of springback caused by elastic recovery) [20]. In addition, consistency in terms of minimization of dimensional variations (caused by variation in lubrication, material properties, or thickness) is a key requirement in mass production [8]-[10].

New challenges arise from the use of new materials. For example, the need to reduce weight in automobiles, and to improve fuel economy, encourages manufacturers to choose lighter and stronger materials (e.g., aluminum and magnesium alloys) in place of steel. However, aluminum and magnesium alloys are not as formable as steel, and produce more springback and fracture problems [1], [2] and [18]. Therefore, a major issue in manufacturing sheet metal products from such materials is the ability to ensure consistent production of good parts, without tears, wrinkling, and minimal spring-back, using a given blank (with specified blank size, sheet thickness, and material properties) and tooling (with specified geometry).

1.2 Motivation

Die design, using the finite element method (FEM) and die try-out, which involves grinding and welding of the die to ensure that the parts produced meet specifications, are

This work was supported by the Michigan Economic Development Corporation (MEDC) under Grant no. 06-1-P1-0084, and the authors gratefully acknowledge the assistance of Troy Design and Manufacturing (TDM) with materials and facilities for the stamping experiments.

Yongseob Lim is a PhD candidate in the Department of Mechanical Engineering at the University of Michigan, Ann Arbor, MI 48109-2125 USA (phone: 734-763-2227; e-mail: limys@umich.edu).

Ravinder Venugopal, PhD, is the president & CTO of Intellicass Inc., Montréal, Canada. He is also an adjunct faculty member at the University of Québec at Montréal, Canada. (e-mail: rvenugopal@intellicass.com).

A. Galip Ulsoy, PhD, is the William Clay Ford Professor of Manufacturing in the Department of Mechanical Engineering, University of Michigan, Ann Arbor, MI 48109-2125 USA (e-mail: ulsoy@umich.edu).

time-consuming tasks. Moreover, engineers in the forming industry also face challenging production problems due to process variability (e.g., variation in material properties and lubrication) [31] and [35]. To improve part quality or correct defects (e.g., wrinkling, tearing, and springback), with given materials and a conventional press, the die geometry is physically modified [34], during die try-out. Both die design and die try-out depend heavily on the experience of experts. Nevertheless, engineers have also been developing standardized procedures for improving part quality in production [24]-[25], [27], [37] and [40].

When it comes to overcoming mass production problems following try-out, new press technologies continuously emerge as new techniques and ideas in sheet metal forming are considered in press design. For example, controlling the flow of sheet metal via controllable multi-cylinder blank holder actuators reduces die-try out time by cutting down on die work (grinding and welding) [4], [5]-[6], [13]-[16], [17], [19]-[21], [33], [36] and [38].

In addition, researchers have developed different types of active blank holder systems (e.g., segmented/pulsating blank holder system and reconfigurable discrete die), to improve stamped part quality in forming [5]-[6], [26], [28], [39] and [41]. A single-input single-out (SISO) process control using a proportional plus integral (PI) controller was investigated based on simple geometry of the die (e.g., *u*-channel forming) under laboratory-based tests [13]-[16], [32] and [41]. However, multi-input multi-output (MIMO) process control to form complex-geometry parts in high volumes has not been studied.

1.3 Purpose and Scope

The focus of this paper is to present a systematic approach to the design and implementation of a MIMO stamping process controller based on complex-geometry parts. The controller corrects blank holder force trajectories obtained from die try-out as process variations occur (e.g., changes in material properties and thickness from batch to batch and lubrication changes). The MIMO controller uses data obtained from four punch force sensors at the 4 corners of the press for a complex-geometry part (e.g., a double-door of a pick-up truck). This paper is based upon original experiments performed with a novel system for binder force control in the stamping process, using 12 hydraulic actuators.

II. Multi-actuator Binder Force Control System

2.1 Experimental System

The experimental system, with twelve hydraulic actuators at the bottom of the die and an Opal-RT real-time data acquisition and control system, is deployed to perform the experiments (see Fig. 2). The complex part used for the experiments is a double-door of a pick-up truck made from a tailor-welded steel blank with three different thicknesses. The press is a 1000 ton mechanical press which can operate at 12 strokes/minute. The material flow is controlled by a set of binders with 12 hydraulic actuators. The punch force at the four corners of the press is measured using full-bridge strain gauges, which are attached to the surface of the four punch-supporting beams on the press (see Fig. 2b). The real-time system plays a key role in controlling the system operation and acquiring the measured data from the sensors. The experimental conditions are given in Table I.

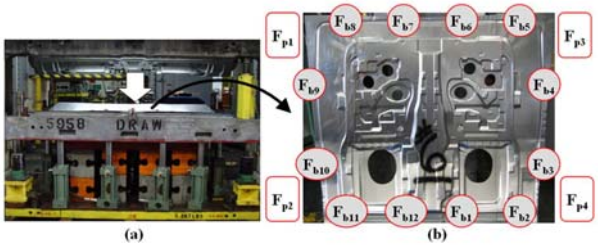

Fig. 2: Experimental system: (a) test die with multiple actuators and blank (b) positions of process variables (top-view).

TABLE I: EXPERIMENTAL CONDITIONS FOR STAMPING

Punch speed, v_p		215 mm/sec
Punch displacement, h_{max}		150 mm
Data sampling rate		0.002 sec (500 Hz)
Lubrication		Dry
Material		CR EDD steel
Blank size		1640 x 1600 x 0.8 mm
Punch force sensor	Type	Full bridge strain gage (120 ~ 1000 Ω)
	Excitation	Built-in 10V@125mA max
	Accuracy	± 1% of full scale max
Binder force sensor	Type	Piezo-resistive strain gage
	Resolution	1 ~ 5V for 0 ~ 2500 psi
Punch stroke sensor	Type	Position transducer
	Accuracy	± 0.005% of full scale

2.2 Implementation of Process Control

Process control is used to ensure that a measurable process variable (i.e., punch force) follows a reference trajectory by manipulating the binder force (see Fig. 3). To implement the process control, a process controller and reference trajectory are required after the monitored process variable (punch force) is selected. The process controller generates reference commands for the machine controller which ensures that the hydraulic actuators provide the desired binder forces, as shown in Fig. 3. For MIMO process control, four reference (or desired) punch force trajectories are determined experimentally by experienced operators. Then, process control is used to make the measured punch forces track these reference punch force trajectories under different lubrication and material property conditions. Thus, process control improves consistency in geometric dimensions and part quality, despite variations in lubrication and material property.

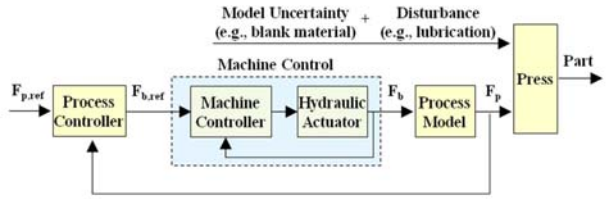

Fig.3: Process control of sheet metal forming process with reference punch force trajectory.

The control-design model of the process must be simple, yet accurate enough to capture the characteristic relationship between the blank holder force and the punch force. A process model mathematically describes the relationship between the binder (or blank holder) force and the punch force, assuming that the punch force generation is a function of the blank holder force; see, for example, where such a model was developed for a single-input single-output (SISO) process and without explicit consideration of the material draw-in during forming [15]. Other researchers have developed sheet metal stamping models based on material flow data from experiments taking into account the local strain [6], [22] and [23].

Such methods, considering both draw-in and local strain of sheet metal, can mathematically determine the elongation of a section of a radial-line out of a drawn part with respect to drawing stroke. However, the relationship between the binder force and the draw-in, or the punch force, including elongation of the sheet metal, has not been investigated.

In our previous work [20] and [21], we described, for the first time, the development of a MIMO linear sheet-metal stamping process model for the purpose of controller design, including elongation of the sheet metal [11]-[12] and [30]. Due to space limitations in this paper, the key features of the model are summarized below.

First, the structures of the process models are shown in Eq. (1) and (2) respectively; one provides the relationship between the actual blank holder force ($F_{b,act}$) as an input and the actual punch force ($F_{p,act}$) as an output, the other provides the whole system structure (G_{total}) which has the relationship between the reference blank holder force ($F_{b,act}$) as an input and the filtered punch force ($F_{p,fil}$) as an output.

$$G_p(z) = \frac{\delta F_{p,act}(z)}{\delta F_{b,act}(z)} = \frac{b_1 z + b_0}{z^2 + a_1 z + a_0} \tag{1}$$

$$G_{total}(z) = \frac{\delta F_{p,fil}(z)}{\delta F_{b,ref}(z)} = G_p(z) \cdot G_m(z) \cdot G_f(z)$$

$$\text{where,} \quad G_m(z) = \frac{\delta F_{b,act}(z)}{\delta F_{b,ref}(z)} = \frac{d_0}{z + c_0} \tag{2}$$

$$G_f(z) = \frac{\delta F_{p,fil}(z)}{\delta F_{p,act}(z)} = \frac{50z}{z - 0.9048}$$

where G_m and G_f represent machine control model (i.e., hydraulic actuator dynamics) and low-pass filter model respectively in experiments. The parameters of these models are obtained from experimental data using the least-squares system identification technique. Furthermore, these models are validated by generating punch force outputs from desired binder force inputs, and comparing them with the directly measured desired punch force outputs.

In addition, we have extended the model in Eq. (2) to the MIMO case by creating a 4 × 12 transfer function matrix (TFM), with 4 punch forces ($\delta F_{p,fil}$) as outputs and 12 binder forces ($\delta F_{b,ref}$) as inputs. Based on the experimentally verified assumption that each punch force output is affected only by three nearest binder force as inputs (see Fig. 2b), we constrain the TFM to a block-diagonal form given by:

$$\begin{bmatrix} \delta F_{p1}(z) \\ \delta F_{p2}(z) \\ \delta F_{p3}(z) \\ \delta F_{p4}(z) \end{bmatrix} = \begin{bmatrix} G_{1,1} & G_{1,2} & G_{1,3} & 0 & 0 & 0 & 0 & 0 & 0 & 0 & 0 & 0 \\ 0 & 0 & 0 & G_{2,4} & G_{2,5} & G_{2,6} & 0 & 0 & 0 & 0 & 0 & 0 \\ 0 & 0 & 0 & 0 & 0 & 0 & G_{3,7} & G_{3,8} & G_{3,9} & 0 & 0 & 0 \\ 0 & 0 & 0 & 0 & 0 & 0 & 0 & 0 & 0 & G_{4,10} & G_{4,11} & G_{4,12} \end{bmatrix} \begin{bmatrix} \delta F_{b1}(z) \\ \delta F_{b2}(z) \\ \vdots \\ \delta F_{b11}(z) \\ \delta F_{b12}(z) \end{bmatrix} \tag{3}$$

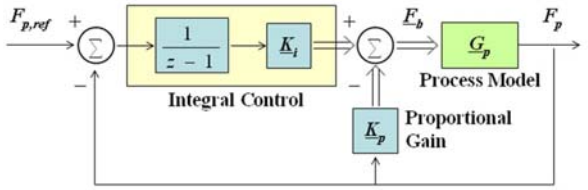

Fig. 4: Block diagram of SIMO PI control system (e.g., $K_p \in R^{1\times 3}$, $K_i \in R^{1\times 3}$ and $G_p \in R^{3\times 1}$).

III. Process Control Design Based on Multi-Input Multi-Output Model

4.1 Design of PI Process Control

For the MIMO system given by the block-diagonal form in Eq. (3), four SIMO proportional plus integral (PI) controllers are implemented using Simulink/Real-Time Workshop® in the experimental system. The block diagram of the SIMO process controller is shown in Fig. 4. The fourth-order linear model, given by a 3 × 1 vector for each single punch force plant output, can be used to design the controller gains, which are given by a 1 × 3 vector for each punch force measurement. To design the PI controller based on the MISO perturbed process model, five steps are followed:

- *Step 1*: Determine PI control gains based on a linear process model by using the root-locus design method. This method shows how PI controller parameters in the system's feedback characteristics influence the pole locations.
- *Step 2*: Investigate the gain margin (GM) and phase margin (PM) using a frequency-response design method (e.g., Bode plot). Based on PI control parameters determined from *Step 1*, stability margins (i.e., GM and

PM) are investigated for several cases described in Table II. It is recommended to provide gain margins not less than 6 dB, and phase margins-not less than π/6 [29]. A sample result of one of the punch forces in Fig. 5, shows a controller design where GM is greater than 60 dB and PM is greater than π/2

- *Step 3*: Check system transient performance (e.g., rise time and settling time) based on three cases of PI control gains determined from *Step 1*, using the closed-loop step response (see Fig. 6). For example, settling time of Case I and Case II is less than 0.05 sec, which satisfies the requirement.
- *Step 4*: Perform simulations based on three cases of PI controller parameters, with experimentally determined reference punch forces. This step is used to assess the tracking performance of the controller while ensuring that the control signals meet the binder force saturation constraints (minimum 0 tons and maximum 16 tons).
- *Step 5*: Perform the experiments with the selected gains for the PI process controller.

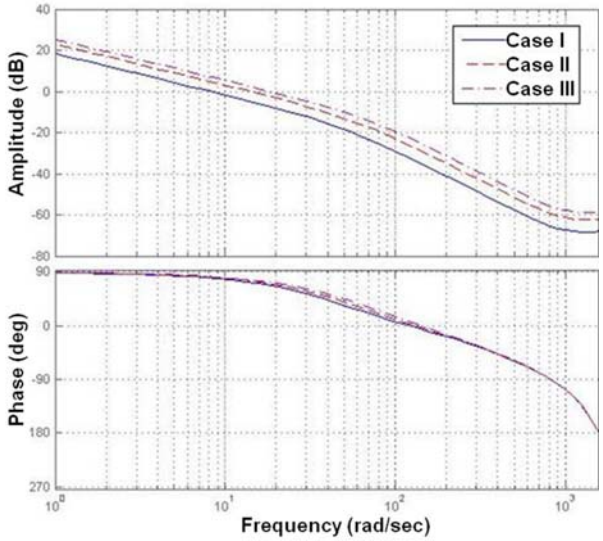

Fig. 5: Bode plot based on the PI control gains for the punch force (i.e., F_{p1}).

4.2 Simulation and Experimental Results

Simulation is used to validate the performance of the proposed PI process controller based on the linear perturbed process model given in equations (1) and (2). The simulation models use the perturbed binder forces ($\underline{\delta F_b}$) as inputs, the perturbed punch force (δF_p) as an output, and the perturbed punch force ($\delta F_{p,ref}$) as the reference. The perturbations are with respect to baseline binder force inputs. The total simulated punch force (F_p), reference punch force ($F_{p,ref}$) and binder forces ($\underline{F_b}$), shown in Fig. 4, are respectively given by

$$\begin{aligned} F_p &= F_{p,base} + \delta F_p \\ F_{p,ref} &= F_{p,base} + \delta F_{p,ref}, \quad F_p \,\&\, F_{p,ref} \in R^1 \end{aligned} \tag{4}$$

$$\underline{F_b} = \underline{F_{b,base}} + \underline{\delta F_b}, \quad \underline{F_b} \in R^{1\times 3} \tag{5}$$

where $F_{p,base}$ is the measured-baseline of the punch force corresponding to the baseline binder forces, $\underline{F_{b,base}}$, which is set to a constant value of 16-tons for all 12 actuators. Fig. 7a shows the simulation results with punch force as output using the PI process controller based on the perturbed linear process model. Based on these simulation results, good experimental tracking performance is expected.

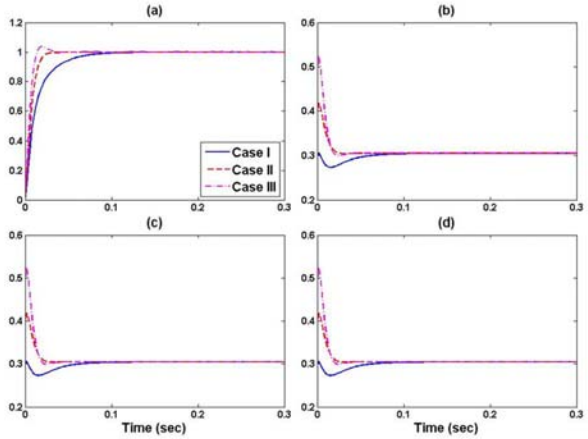

Fig. 6: Simulation results with step input for the punch force #1 (i.e., F_{p1}): (a) output #1 (F_{p1}) (b) input #1 (F_{p7}) (c) input #2 (F_{p8}) (d) input #3 (F_{p9}).

TABLE II: CASES OF SIMULATION AND EXPERIMENT

	Plant model	Cases	$\underline{K_p}$ gains (1 x 3)	$\underline{K_i}$ gains (1 x 3)
Simulation	All models (δF_{p1} - δF_{p4})	Case I	[0.3 0.3 0.3]	[0.01 0.01 0.01]
		Case II	[0.4 0.4 0.4]	[0.02 0.02 0.02]
		Case III	[0.5 0.5 0.5]	[0.03 0.03 0.03]
Experiment	F_{p1}	Experiment cases	[0.4 0.2 0.6]	[0.01 0.01 0.01]
	F_{p2}		[0.1 0.15 0.15]	[0.01 0.01 0.01]
	F_{p3}		[0.6 0.2 0.4]	[0.01 0.01 0.01]
	F_{p4}		[0.15 0.15 0.1]	[0.01 0.01 0.01]

Fig. 7b shows simulation and experimental results for the three binder force inputs (i.e., F_{b7}, F_{b8} & F_{b9}) associated with each punch force output (i.e., F_{p1}). Although there is variation in the binder forces, the simulated binder force trajectories are similar to the measured binder force trajectories.

Experimental results for one of four punch force outputs (i.e., F_{p1}), using the MIMO PI process controller and the reference punch force trajectory, is shown in Fig. 8. Consequently, Fig. 9 shows the effect of binder force control on part quality for a double-door with complex geometry made from a tailor-welded blank; Firstly, Fig. 9b shows that wrinkling occurs when the binder forces for all 12 actuators are commanded to the constant baseline value of 8 tons. Secondly, Fig. 9c shows that a split occurs when the binder forces for all 12 actuators are commanded to a constant value of 16 tons. Finally, Fig. 9a shows that MIMO process control eliminates these defects. The MIMO process controller adjusts the binder forces, which have been

initially commanded to a constant value of 16 tons, to track the reference punch force trajectories. Thus, the MIMO process control corrects the defects by appropriately regulating the material flow. This indicates that the MIMO process controller works well.

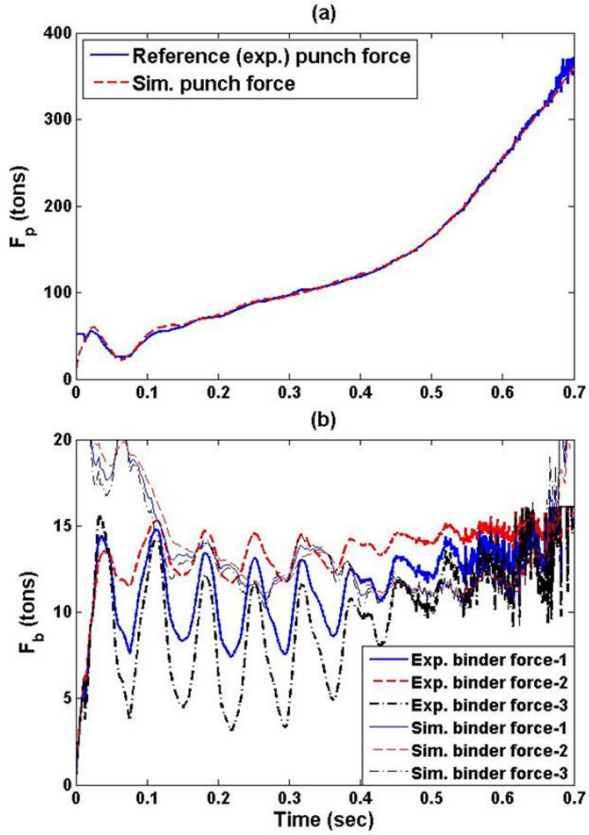

Fig. 7: Simulation and experimental results: (a) simulation results of punch force (i.e., F_{p1}) (b) comparison of three binder forces (F_{b7}, F_{b8} & F_{b9}) for punch force (i.e., F_{p1}) between experiment and simulation.

IV. Discussion and Remarks

The MIMO PI process controller has 24 parameters, namely, 12-proportional gains and 12-integral gains. The MIMO PI process control (i.e., output feedback control) is simple compared to other control design methods (e.g., pole placement and LQ design method based on state feedback control) and also works well to improve part quality (shown in Fig. 9). However, trial-and-error controller tuning is time consuming and thus, auto-tuning methods will be investigated. Future work will also consider combining auto-tuning with iterative learning control (ILC) or adaptive control.

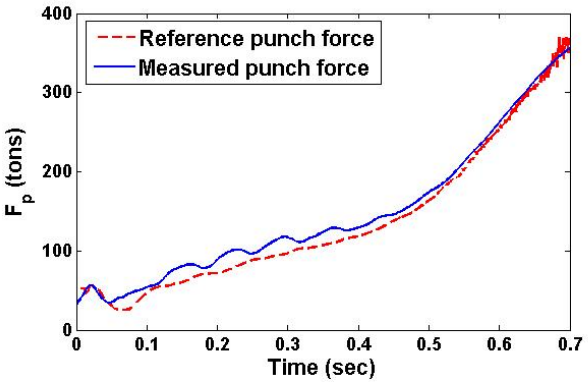

Fig. 8: Experimental results of punch force (i.e., F_{p1}) as output tracking reference punch force

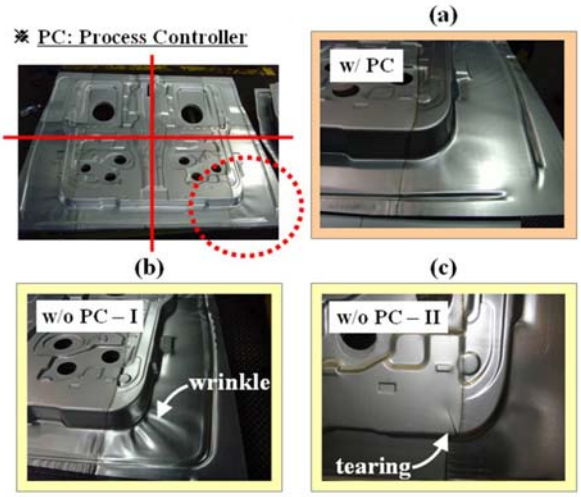

Fig. 9: Improved part quality comparisons: (a) with PC, (b) without PC for constant 8-ton binder force (c) without PC for constant 16-ton binder force for complex part geometry (i.e., double-door panel)

V. Summary and Conclusion

The MIMO stamping process control has been shown to improve part quality and consistency for a complex-geometry part. For the first time, a MIMO PI stamping process controller with good tracking performance has been developed and experimentally validated. However, controller tuning based on trial-and-error in experimental tests is time consuming and expensive. Future work will investigate auto tuning methodologies.

Acknowledgment

The authors gratefully acknowledge the financial support provided by the Michigan Economic Development Corporation under Grant no. 06-1-P1-0084, and the assistance of Troy Design and Manufacturing (TDM) with materials and facilities for the stamping experiments.

REFERENCES

[1] Adamson, A. Ulsoy, A.G., Demeri, M., 1996, "Dimensional Control in Sheet Metal Forming via Active Binder Force Adjustment," *SME Transactions*. Vol. 24, pp. 167-178.

[2] Anon, 2006, "Heavier than ever, but lighter inside," *AutoTechnology*, Vol. 6, pp. 30-33.

[3] Astrom, Karl J., Wittenmark, Bjorn, 1990, "Computer-Controlled Systems," *Prentice Hall*, pp. 416-436.

[4] Bohn, Stefen U. Jurthe, Weinmann, Klaus J., 1998, "A New Multi-point Active Drawbead Forming Die: Model Development for Process Optimization," *SAE Paper* No. 980076, pp. 24-30.

[5] Doege, E., Elend, L.E., 2001, "Design and application of pliable blank holder systems for the optimization of process conditions in sheet metal forming," *J of Materials Proc. Tech*. Vol 111, pp. 182-187.

[6] Doege, E., Schmidt-Jurgensen, R., Huinink, S., Yun, J.-W, 2003, ''Development of an optical sensor for the measurement of the material flow in deep drawing processes," *CIRP Annals - Manufacturing Technology*, Vol 52, n1, pp. 225-228.

[7] Doege, E., Seidel, H.J., Griesbach, B., Yun, J.W., 2002, "Contactless on-line measurement of material flow for closed loop control of deep drawing," *J of Materials Proc. Tech*. 130–131, pp. 95–99.

[8] Hardt, D. E., 1993, "Modeling and Control of Manufacturing Processes: Getting More Involved," *J. of Dynamic Systems, Measurement, and Control*, Vol. 115, pp. 291–300.

[9] Hardt, D. E., Fenn, R. C., 1993, ''Real-Time Control of Sheet Stability during Forming,'' *J. of Dynamic Systems, Measurement, and Control*, Vol. 115, pp. 301–308.

[10] Hardt, D. E., Contantine, E., Wright, A., 1992, "A Model of the Sequential Bending Process for Manufacturing Simulation," *J. of Eng. for Industry*, Vol. 114, pp. 181-187.

[11] Hollomon, J.H., 1945, "Plastic Flow of Metals," Metal Tech., Vol. 12.

[12] Hosford, W.F., Caddell, R.M., 2007, "Metal Forming: Mechanical and Metallurgy," *Cambridge University Press*, pp. 52-65.

[13] Hsu, C.W., Ulsoy, A.G., Demeri, M.Y., 2002, "Development of process control in sheet metal forming," *J. of Materials Proc. Tech*. Vol. 127, pp. 361-368.

[14] Hsu, C.W., Ulsoy, A.G., Demeri, M.Y., 2000, "An Approach for Modeling Sheet Metal Forming for Process Controller Design," *ASME J. Manuf. Sci. Eng*. 122, pp. 717-724.

[15] Hsu, C.W., Ulsoy, A.G., Demeri, M.Y., 1999, "Process Controller Design for Sheet Metal Forming," *American Control Conference*, Vol.1, pp. 192 – 196.

[16] Hsu, C.W., Ulsoy, A.G., Demeri, M.Y., 2000, "Application of Real-Time Process Control in Sheet Metal Forming," *Proceedings of the 2000 Japan–USA Symposium*.

[17] Kergen, R., Jodogne, P., 1992, "Computerized Control of the Blankholder Pressure on Deep Drawing Process," *SAE Paper* No. 920433, pp. 51-55.

[18] Lee, Y.S., Kim, M.C., Kim, S.W., Kwon, Y.N., Choi, S.W., Lee, J.H., 2007, "Experimental and Analysis Studies for Forming Limit of AZ31 Alloy on Warm Sheet Metal Forming," *J. of Materials Processing Tech*., Vol. 187-188, pp. 103-107.

[19] Lim, Y.S., Venugopal, R. Ulsoy, A.G., 2008a, "Advances in the Control of Sheet Metal Forming," *Proceeding of IFAC*, 2008. Seoul, Korea.

[20] Lim, Y.S., Venugopal, R. Ulsoy, A.G., 2008b, "A Multi-Input Multi-Output Model for Stamping Process Control," *Proceeding of ISFA*, 2008. Atlanta, Georgia.

[21] Lim, Y.S., Venugopal, R. Ulsoy, A.G., 2009, "Multi-Input Multi-Output Modeling and Control for Stamping," *J. of Dynamic Systems, Measurement, and Control*, submitted for publication

[22] Lo, Sy-Wei, Jeng, Guo-Ming, "Monitoring the Displacement of a Blank in a Deep Drawing Process by Using a New Embedded-Type Sensor," *Int J Adv Manuf Tech*., vol. 15, pp. 815–821.

[23] Mahayotsanun, N., Cao, J., Peshkin, M., 2005, "A Draw-In Sensor for Process Control and Optimization," *American Institute of Physics*, CP778 Vol. A.

[24] Manabe, K., Koyama, H., Katoh, K., Yoshihara, S., 1999, "Intelligent Design Architecture for Process Control of Deep-Drawing," *Intelligent Processing and Manufacturing of Materials*, Vol. 1, pp. 571-576.

[25] Manabe, K., Koyama, H., Katoh, K., Yoshihara, S., Yagami, T., 2002, "Development of a combination punch speed and blank-holder fuzzy control system for the deep-drawing process," *J of Materials Proc. Tech*. 125–126, pp. 440–445.

[26] Michler, J.R., Weinmann, K.J., Kashani, A.R., Majlessi, S.A., 1994, "A Strip drawing simulator with computer-controlled drawbead penetration and blankholder pressure," *J. Materials Proc. Tech*., Vol. 43, pp. 177-194.

[27] Obermeyer, E.J., Majlessi, S.A., 1997, "A review of recent advances in the application of blank-holder force towards improving the forming limits of sheet metal parts," *J. Materials Proc. Tech*., Vol. 75, pp. 222-234.

[28] Rzepniewski, Adam K., Hardt, D.E., 2004, "Multi input-Multi Output Cycle-To-Cycle Control of Manufacturing Processes," *3rd Annual SMA Symposium*, Singapore.

[29] Safonov, Michael G., 1980, "Stability and Robustness of Multivariable Feedback Systems," *MIT press*.

[30] Shaw, M.T., MacKnight, W.J., 2005 "Introduction to Polymer Viscoelasticity," *Wiley-Interscience*, 2005.

[31] Sheng, Z. G., Jirathearnat, S., Altan, T., 2004, "Adaptive FEM Simulation for Prediction of Variable Blank Holder Force in Conical Cup Drawing," *International J. of Machine Tools & Manuf*, Vol. 44, pp. 487–494.

[32] Siegert, K., Hohnhaus, J., Wagner, S., 1998, "Combination of Hydraulic Multipoint Cushion System and Segment-Elastic Blankholders," *SAE Paper* No. 98007, pp. 51-55.

[33] Siegert, K., Ziegler, M., Wagner, S., 1997, "Loop Control of the Friction Force: Deep drawing process," *J. of Materials Proc. Tech*. Vol. 71, pp. 126-133.

[34] Sklad, M.P., Harris, C.B., Slekirk, J.F., Grieshaber, D.J., 1992, "Modeling of Die Tryout," SAE Paper No. 920433, pp. 151-157.

[35] Sunseri, M., Cao, J., Karafillis, A.P., Boyce, M.C., 1996, "Accommodation of Springback Error in Channel Forming Using Active Binder Force: Control Numerical Simulations and Experiments," *J. of Engin. Materials and Tech*. Vol. 118, pp. 426-435.

[36] Wang, L., Lee, T.C., 2005, "Controlled strain path forming process with space variant blank holder force using RSM method," *J. of Materials Processing Tech*., Vol. 167, pp. 447–455.

[37] Webb, R.D., Hardt, D.E., 1991, "A Transfer Function Description of Sheet Metal Forming for Process Control," *Trans. ASME, J. Eng. Ind.*, Vol. 113, pp. 44-52.

[38] Xu, S., Zhao, K., Lanker, T., Zhang, J., Wang, C.T., 2007, "On Improving the Accuracy of Springback Prediction and Die Compensation," *SAE Paper* No. 2007-01-1687.

[39] Yagami, T., Manabe, Ken-ichi, Yang, M., Koyama, H., 2004, "Intelligent Sheet Stamping Process Using Segment Blankholder Modules," *J. of Materials Proc. Tech*. Vol. 155–156, pp. 2099–2105.

[40] Zhang, S.J., Aitharaju, J., Wu, V.W., Zhao, K., Wang, C., 2005, "Virtual Manufacturing of Automotive Body Side Outers Using Advanced Line Die Forming Simulation," *AIP Conference Proceedings*, n778, pt.1, pp. 867-72.

[41] Ziegler, M., 1999, "Pulsating Blankholder Technology," *SAE Paper* No. 1999-01-3155, pp. 1-5.